Journal of Holography Applications in Physics
Volume 3, Issue 2, Spring 2023, 59-67
©Available online at http://jhap.du.ac.ir
DOI:10.22128/jhap.2023.675.1049
Online ISSN: 2783-3518

Journal of Holography Applications in Physics

Regular article

Hairy AdS black holes with Robin boundary conditions

Takaaki Ishii
Department of Physics, Rikkyo University, Nishi-Ikebukuro, Toshima, Tokyo 171-8501, Japan;
Email: ishiitk@rikkyo.ac.jp

Received: April 18, 2023; Revised: May 01, 2023; Accepted: May 21, 2023.

Abstract. We study hairy black holes in Einstein-Maxwell-complex scalar theory in four-dimensional asymptotically global anti-de Sitter (AdS) spacetime when the Robin boundary conditions are imposed on the scalar field. The hairy solutions branch from the Reissner-Nordström-AdS (RNAdS) black holes at the onset of instability of the scalar field under the Robin boundary conditions. There are also associated horizonless solutions called boson stars. Comparing thermal AdS, RNAdS, charged boson stars, and hairy black holes, we obtain phase diagrams in the grand canonical ensemble.

Keywords: Holography; Black Holes; Holographic Superconductivity.

1 Introduction

The Einstein-Maxwell-complex(charged) scalar system in asymptotically anti-de Sitter (AdS) spacetime is known to show the spontaneous breaking of the $U(1)$ gauge symmetry, discussed as the appearance of the superfluid/superconducting phase [1, 2]. This is often considered with the so-called Dirichlet boundary conditions on the scalar field at the AdS boundary. However, when the field has a mass close to the Breitenlohner-Freedman bound [3, 4], general conditions known as the Robin boundary conditions (also called mixed boundary conditions) can be imposed. It is also known that the Robin boundary conditions can also make the AdS spacetime unstable [5]. There is hence interplay of instabilities whose origins are different. In [6], linear perturbations of the four-dimensional Reissner-Nordström AdS (RNAdS) spacetime with global AdS asymptotics were studied for the scalar field with Robin boundary conditions, and instability was discussed. In this talk, we discuss hairy black holes that branch from the RNAdS by taking into account the backreaction of the instability [7]. In global AdS asymptotics, related horizonless hairy solutions called boson stars can be also obtained. By comparing horizonless and black hole solutions, we find rich phase structure of solutions with nontrivial scalar field under the Robin boundary conditions.

2 Instability of the RNAdS black hole

We consider Einstein-Maxwell-complex scalar theory in four-dimensional asymptotically global AdS spacetime. The action is

$$S = \frac{1}{8\pi G_N}\int \mathrm{d}^4x\sqrt{-g}\left(\frac{1}{2}\left(R-2\Lambda\right)-\frac{1}{4}F_{\mu\nu}F^{\mu\nu}-|D\phi|^2-m^2|\phi|^2\right), \tag{1}$$

where $F_{\mu\nu}=\partial_\mu A_\nu-\partial_\nu A_\mu$ and $D_\mu\phi=\partial_\mu\phi-iqA_\mu\phi$. The gauge coupling constant is written by q. We set $\Lambda=-3$ and $m^2=-2$ (The AdS radius is unity). We study spherically symmetric static solutions in the spherical $R\times S^2$ AdS boundary. The ansatz is given by

$$\mathrm{d}s^2 = -\left(1+r^2\right)f(r)e^{-\chi(r)}\mathrm{d}t^2+\frac{\mathrm{d}r^2}{\left(1+r^2\right)f(r)}+r^2\mathrm{d}\Omega_2^2, \tag{2}$$

$$A = A_t(r)\mathrm{d}t, \qquad \phi=\phi(r). \tag{3}$$

When $f(r)=1$, $\chi(r)=0$ (and $A=\phi=0$), we obtain the empty AdS called *thermal AdS*.

This system also allows the RNAdS black hole solution given by

$$\begin{aligned}\left(1+r^2\right)f(r) &= 1+r^2-\left(1+r_h^2+\frac{Q^2}{2r_h^2}\right)\frac{r_h}{r}+\frac{Q^2}{2r^2},\\ A_t(r) &= \mu-\frac{Q}{r}, \quad \chi(r)=\phi(r)=0,\end{aligned} \tag{4}$$

where r_h denotes the location of the outermost horizon, satisfying $f(r_h)=0$, and μ and Q are the $U(1)$ chemical potential and charge density. We use a gauge in which $A_t(r_h)=0$. If $\mu^2<2$, the first order transition known as the Hawking-Page transition occurs between the RNAdS and thermal AdS in the grand canonical ensemble when [8, 9, 10]

$$T_{\mathrm{HP}} = \frac{\sqrt{2-\mu^2}}{\sqrt{2}\,\pi}. \tag{5}$$

If $\mu^2>2$, the RNAdS black hole becomes extremal (the temperature becomes zero) when

$$\mu=\sqrt{2(1+3r_h^2)}\equiv\mu_{\mathrm{ext}}. \tag{6}$$

We wish to see when ϕ can be nonzero. To search the onset of instability of ϕ, it is sufficient to assume a static perturbation. The static perturbation equation is given by

$$\phi''(z)+\left(\frac{F'}{F}-\frac{2}{z}\right)\phi'(z)-\left(\frac{m^2}{z^2F}-\frac{q^2A_t^2}{F^2}\right)\phi(z)=0, \tag{7}$$

where $m^2=-2$ and we use a new coordinate $z\equiv 1/r$ and $F(z)\equiv(1+z^2)f(z)$. The asymptotic behavior of ϕ in $z\to 0$ takes the form

$$\phi=\phi_1 z+\phi_2 z^2+\cdots, \tag{8}$$

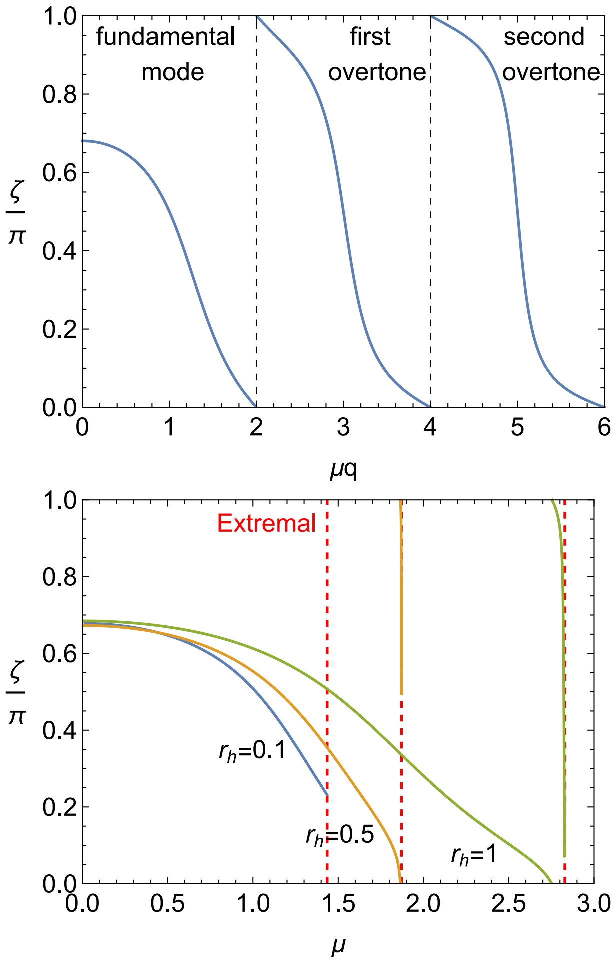

Figure 1: (a) Top: The charged scalar field normal modes of global AdS with constant $A_t = \mu$; $r_h = 0$. (b) Bottom: The onset of instability of the RNAdS for $r_h = 0.1, 0.5, 1$ at $q = 1$.

where both of ϕ_1 and ϕ_2 can be nonzero as normalizable normal modes. For solving Eq.(7), we impose Robin boundary conditions at the AdS boundary $z = 0$. The Robin boundary conditions can be specified by a parameter ζ defined by

$$\cot\zeta = \frac{\phi_2}{\phi_1}, \tag{9}$$

where we choose the domain of ζ as $0 \leq \zeta < \pi$. The points $\zeta = 0$ and $\zeta = \pi/2$ correspond to the Dirichlet and Neumann boundary conditions, respectively.

Under the Robin boundary conditions, we search the onset of instability for the scalar field perturbation in the four-dimensional parameter space (ζ, r_h, μ, q). In figure 1, we show (a) the location of the AdS charged scalar field normal modes (i.e. for $r_h = 0$) and (b) the onset of instability of the RNAdS for $r_h = 0.1, 0.5, 1$ at $q = 1$. In figure 1 (b), the value of μ is bounded from above by extremality as $\mu \leq \mu_{\rm ext}$ given in Eq.(6), which is marked by the vertical red dashed line for each r_h. In this figure, the RNAdS is unstable to the charged scalar field perturbation above each curve, which can be found by studying full quasinormal modes by including nonzero frequencies as $e^{-i\omega t}$ (see also [6]). Correspondingly, also in figure 1 (a), nonzero scalar field solutions will exist in the region upper from the curve. In the following, we wish to discuss backreacted solutions in these regions.

3 Hairy black holes

Knowing the onset of instability for the charged scalar field perturbation of the RNAdS, we will construct backreacted hairy black hole solutions branching at the onset of instability. With the ansatz Eq.(2), the equations of motion are given by coupled ODEs for $f(z) = F(z)/(1+z^2), \chi(z), \phi(z), A_t(z)$ as

$$F' - \left(\frac{3}{z} + z\phi'^2\right) F - e^{\chi}\left(\frac{z^3 A_t'^2}{2} + \frac{zq^2 A_t^2 \phi^2}{F}\right) + z + \frac{3}{z} + \frac{2\phi^2}{z} = 0, \tag{10}$$

$$\chi' - 2z\phi'^2 - \frac{2ze^{\chi} q^2 A_t^2 \phi^2}{F^2} = 0, \tag{11}$$

$$\phi'' + \left(\frac{F'}{F} - \frac{\chi'}{2} - \frac{2}{z}\right) + \left(\frac{2}{z^2 F} + \frac{e^{\chi} q^2 A_t^2}{z^2 F}\right)\phi = 0, \tag{12}$$

$$A_t'' + \frac{\chi'}{2} A_t' - \frac{2q^2\phi^2}{z^2 F} A_t = 0. \tag{13}$$

In the AdS boundary $z = 0$, these equations can be solved asymptotically by

$$f(z) = 1 + \phi_1^2 z^2 + f_3 z^3 + \cdots, \tag{14}$$

$$\chi(z) = \chi_0 + \phi_1^2 z^2 + \cdots, \tag{15}$$

$$\phi(z) = \phi_1 z + \phi_2 z^2 + \cdots, \tag{16}$$

$$A_t(z) = a_0 + a_1 z + \cdots, \tag{17}$$

where $(f_3, \chi_0, \phi_1, \phi_2, a_0, a_1)$ are six integration coefficients that are not determined in the asymptotic analysis. Among these, we can set $\chi_0 = 0$ by a scaling symmetry so that the behavior of the metric Eq.(2) in $z \to 0$ becomes

$$\mathrm{d}s^2|_{z\to 0} = \frac{1}{z^2}\left(-\mathrm{d}t^2 + \mathrm{d}z^2 + \mathrm{d}\Omega_2^2\right). \tag{18}$$

In the bulk, we impose the presence of the black hole horizon at $z = 1/r_h$, or regularity at the center of AdS ($z = \infty$) if we consider horizonless solutions that can be obtained in the same ansatz.

The asymptotic coefficients in Eqs.(14)–(17) are related to thermodynamic quantities. Carrying out the holographic renormalization, we obtain the expressions of the thermodynamic quantities in terms of the asymptotic coefficients. For the Robin boundary conditions, the scalar field is dual to the dimension 1 operator $\mathcal{O}_1$. The expression of the total energy, charge, and scalar expectation value for the Robin boundary conditions is

$$\begin{aligned} \mathcal{E} &= 4\pi(-f_3 + 3\phi_1^2 \cot\zeta) = 4\pi(-f_3 + 3\phi_1\phi_2), \\ \mathcal{Q} &= -4\pi a_1, \qquad \langle \mathcal{O}_1 \rangle = 4\pi\sqrt{2}\,\phi_1. \end{aligned} \tag{19}$$

The chemical potential conjugate to $\mathcal{Q}$ is given by $\mu = a_0$. We also have the Hawking temperature T_{H} and entropy $\mathcal{S}_{\mathrm{BH}} \equiv 8\pi^2 r_h^2$. The first law of thermodynamics/black hole

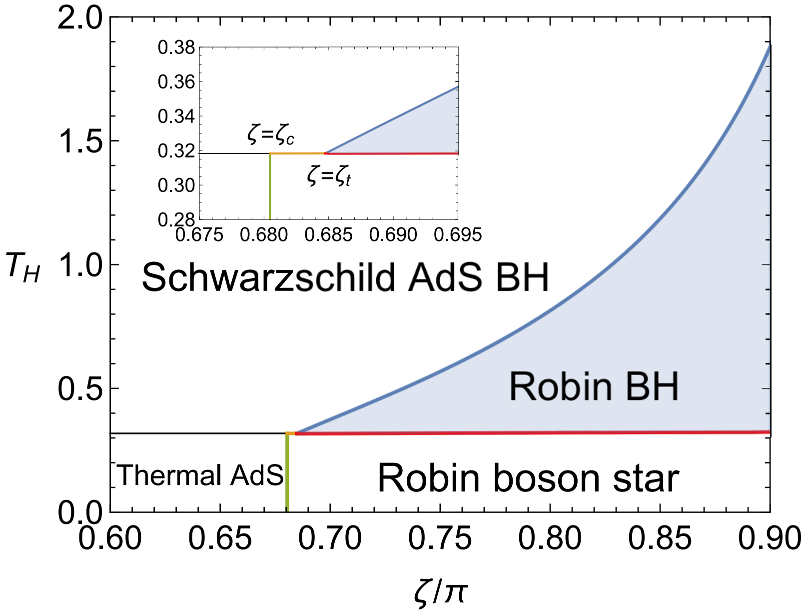

Figure 2: The phase diagram for neutral solutions.

mechanics for these thermodynamic quantities are given by

$$d\mathcal{E} = T_{\rm H} d\mathcal{S}_{\rm BH} + \mu d\mathcal{Q} + \frac{1}{8\pi}\langle\mathcal{O}_1\rangle^2 d(\cot\zeta), \tag{20}$$

where we also included the variation of the parameter of the Robin boundary condition ζ. The grand potential for the grand canonical ensemble is given by

$$\Omega = \mathcal{E} - T_{\rm H}\mathcal{S}_{\rm BH} - \mu\mathcal{Q}. \tag{21}$$

4 Results

4.1 Neutral boson stars and black holes

When the gauge field is absent, the phase structure is specified by two parameters $(T_{\rm H}, \zeta)$. In this case, the free energy we compare is the grand potential Eq.(21) at $\mu = 0$, $\Omega|_{\mu=0} = (\mathcal{E} - T_{\rm H}\mathcal{S}_{\rm BH})_{\mu=0}$. We compare the free energies among thermal AdS, Schwarzschild AdS, horizonless geometry with nonzero neutral scalar, which we call *Robin boson stars*, and black holes with neutral scalar hair, which we call *Robin black holes*.

The neutral phase diagram is shown in figure 2. The blue line at the border of the Schwarzschild AdS and hairy Robin black holes is the second order phase transition for growing scalar hair, and it extends in

$$\zeta \geq \zeta_t \simeq 0.6847\pi. \tag{22}$$

As ζ increases, the critical temperature for this scalar hair formation rises, and in the limit $\zeta \to \pi$ ($\cot\zeta \to -\infty$), the Robin black holes dominate at any high temperatures. The vertical green line is the second order phase transition from thermal AdS to Robin boson stars, and it is located at

$$\zeta = \zeta_c = \pi - \tan^{-1}(\pi/2) \simeq 0.6805\pi. \tag{23}$$

The red line in $\zeta \geq \zeta_t$ marks the first order Hawking-Page transition between Robin black holes and Robin boson stars. The short orange segment in $\zeta_c \leq \zeta \leq \zeta_t$ (see the inset) is the first order phase transition between Schwarzschild AdS and Robin boson stars; for ζ in this region, Robin black holes have the higher free energy than these two, and hence the first order phase transition is between the Schwarzschild AdS and Robin boson stars. The red, orange, and blue lines merge at $\zeta = \zeta_t$, where

$$T_{\rm H} \simeq 0.3184. \tag{24}$$

This is slightly higher than the transition temperature $T_{\rm HP}$ for the Schwarzschild AdS and thermal AdS Eq.(5), $T_{\rm HP}|_{\mu=0} = 1/\pi \simeq 0.3183$. Also in $\zeta > \zeta_t$, the Hawking-Page transition temperature depends on ζ very mildly. We were not able to pin down the line of the Hawking-Page transition up to $\zeta \to \pi$ because of numerical limitations. But, as long as we could confirm, the transition temperature (red line) behaves as

$$T_{\rm H} \simeq 0.03(\zeta - \zeta_t)/\pi + 0.3184. \tag{25}$$

4.2 Charged boson stars and black holes

In the presence of the gauge field, we consider black holes with nontrivial charged scalar field with the Robin boundary conditions. We call these *hairy Robin black holes*. The associated charged but horizonless solutions with the Robin boundary conditions will be called *charged Robin boson stars*. The phase space depends on the all four parameters $(\mu, T_{\rm H}, \zeta, q)$. The grand potential of charged Robin boson stars always satisfies $\Omega < 0$, while thermal AdS has $\Omega = 0$. Therefore, the charged Robin boson stars are always preferred over the thermal AdS when the two solutions overlap.

In figure 3, phase diagrams are shown for $q = 1$ and different ζ. In each figure, the blue line on the border between the RNAdS and hairy Robin black holes denotes the second-order phase transition below which the scalar hair forms. The vertical green line is for the second-order phase transition between thermal AdS and charged Robin boson stars. The red line is the first order Hawking-Page transition between hairy Robin black holes and charged Robin boson stars. The orange segment denotes the first order phase transition between the RNAdS and charged Robin boson stars. The black dashed line is plotted for reference of the Hawking-Page transition between the thermal AdS and RNAdS Eq.(5), although it is not physically dominant because it is superseded by the charged Robin boson star phase.

Starting from a large value of ζ, we list notable features in the phase structure by decreasing ζ.

- $\zeta > \zeta_t \simeq 0.6847\pi$: In figure 3 (a), neutral solutions ($\mu = 0$) can have nontrivial scalar hair in this region of ζ. Thermal AdS does not appear in any μ because its free energy is always higher than neutral Robin boson stars when these geometries overlap. Hence, the phase diagram consists of three phases: RNAdS, hairy Robin black holes, and charged Robin boson stars. By decreasing the temperature, the RNAdS spontaneously grows the scalar hair, and then there is the first order transition between the black holes and boson stars. This feature is common to all μ.

- $\zeta_t > \zeta > \zeta_c \simeq 0.6805\pi$: In figure 3 (b), the phase structure for this parameter region is shown for $\zeta/\pi = 0.682$. When $\zeta = \zeta_t$, the two phase transition lines (blue and red) first meet at $\mu = 0$. In $\zeta < \zeta_t$, the phase transition from the RNAdS to charged Robin boson stars (orange line) appears, where the hairy Robin black holes have the higher grand potential than the other two.

- $\zeta_c > \zeta \gtrsim 0.24\pi$: The phase diagram in this parameter region is shown in figure 3 (c). In $\zeta < \zeta_c$, the thermal AdS phase can be present as μ is increased from 0 until the charged Robin boson stars branch from thermal AdS (vertical green line).

- In figures 3 (a)–3 (c), the Hawking-Page transition (red line) will approach $T_{\rm H} \to 0$ as μ is increased. We were not able to compute up to this limit due to tough numerics, but we can see that the transition line will go down towards $T_{\rm H} \to 0$ for a wide parameter range.

- $\zeta \simeq 0.24\pi$: When ζ is decreased further, the Hawking-Page transition between hairy Robin black holes and charged Robin boson stars reaches zero temperature and disappears. Figure 3 (d) is the phase diagram for $\zeta/\pi = 0.239$. This has four phases, but the charged Robin boson stars and hairy Robin black holes are separated by the RNAdS, and correspondingly there is a small gap of μ at zero temperature where the extremal RNAdS survives in the phase diagram, and the charged hairy Robin black holes branch from the extremal RNAdS.

- $\zeta \lesssim 0.24\pi$: The charged Robin boson star phase disappears when ζ is decreased further. In figure 3 (e), the phase diagram is shown at $\zeta/\pi = 0.2$. While the charged Robin boson stars can be also obtained as solutions, their grand potential is always bigger than that of RNAdS and hairy Robin black holes, and hence they do not show up in the grand canonical phase diagram.

When the coupling q is increased, the ζ dependence of the phase structure is affected. For $q \geq \sqrt{2}$, the phase structures of figures 3 (d) and 3 (e) are absent. No extremal RNAdS is stable against scalar hair formation even for the Dirichlet boundary condition $\zeta = 0$. For $q = \sqrt{2}$ and $\zeta = 0$, a phase structure not shown here appears (see figure 7(a) in [11]). For $q > \sqrt{2}$ and any ζ, the scalar hair grows at finite temperatures before extremality is reached.

5 Conclusion

We considered charged boson stars and black holes in four-dimensional Einstein-Maxwell-complex scalar theory in asymptotically global AdS spacetime when the Robin boundary conditions are imposed on the charged scalar field. This setup has the four-dimensional parameter space $(T_{\rm H}, \mu, q, \zeta)$, and allowing the Robin boundary conditions offers the most general static spherical solutions in the four-dimensional Einstein-Maxwell-complex scalar theory. The phase structure and phase transition are studied in the grand canonical ensemble. There are four phases characterized by the presence and absence of the black hole horizon and nontrivial scalar hair. There is an interplay between two kinds of instability on the formation of a charged scalar hair, the one caused by the Robin boundary conditions and the other by the $U(1)$ charge of the black hole geometry. These introduce the richer phase structure, compared with the case of the Dirichlet boundary condition.

Data Availability

No data are available.

Conflicts of Interest

The author declares that there is no conflict of interest.

Ethical Considerations

The author has diligently addressed ethical concerns, such as informed consent, plagiarism, data fabrication, misconduct, falsification, double publication, redundancy, and other related matters.

Acknowledgment

The work of T.I. was supported in part by JSPS KAKENHI Grant Number 19K03871.

References

[1] S.A. Hartnoll, C.P. Herzog and G.T. Horowitz, "Building a Holographic Superconductor", Phys. Rev. Lett. **101**, 031601 (2008).

[2] S.A. Hartnoll, C.P. Herzog and G.T. Horowitz, "Holographic Superconductors", JHEP **12**, 015 (2008).

[3] P. Breitenlohner and D.Z. Freedman, "Positive Energy in anti-De Sitter Backgrounds and Gauged Extended Supergravity", Phys. Lett. B **115**, 197 (1982).

[4] P. Breitenlohner and D.Z. Freedman, "Stability in Gauged Extended Supergravity", Annals Phys. **144**, 249 (1982).

[5] A. Ishibashi and R.M. Wald, "Dynamics in nonglobally hyperbolic static space-times. 3. Anti-de Sitter space-time", Class. Quant. Grav. **21**, 2981 (2004).

[6] T. Katagiri and T. Harada, "Stability of small charged anti-de Sitter black holes in the Robin boundary", Class. Quant. Grav. **38**, 135026 (2021).

[7] T. Harada, T. Ishii, T. Katagiri and N. Tanahashi, "Hairy black holes in AdS with Robin boundary conditions", arxiv.org/abs/2304.02267

[8] S.W. Hawking and D.N. Page, "Thermodynamics of Black Holes in anti-De Sitter Space", Commun. Math. Phys. **87**, 577 (1983).

[9] E. Witten, "Anti-de Sitter space, thermal phase transition, and confinement in gauge theories", Adv. Theor. Math. Phys. **2**, 505 (1998).

[10] A. Chamblin, R. Emparan, C.V. Johnson and R.C. Myers, "Holography, thermodynamics and fluctuations of charged AdS black holes", Phys. Rev. D **60**, 104026 (1999).

[11] P. Basu, C. Krishnan and P.N. Bala Subramanian, "Phases of Global AdS Black Holes", JHEP **06**, 139 (2016).

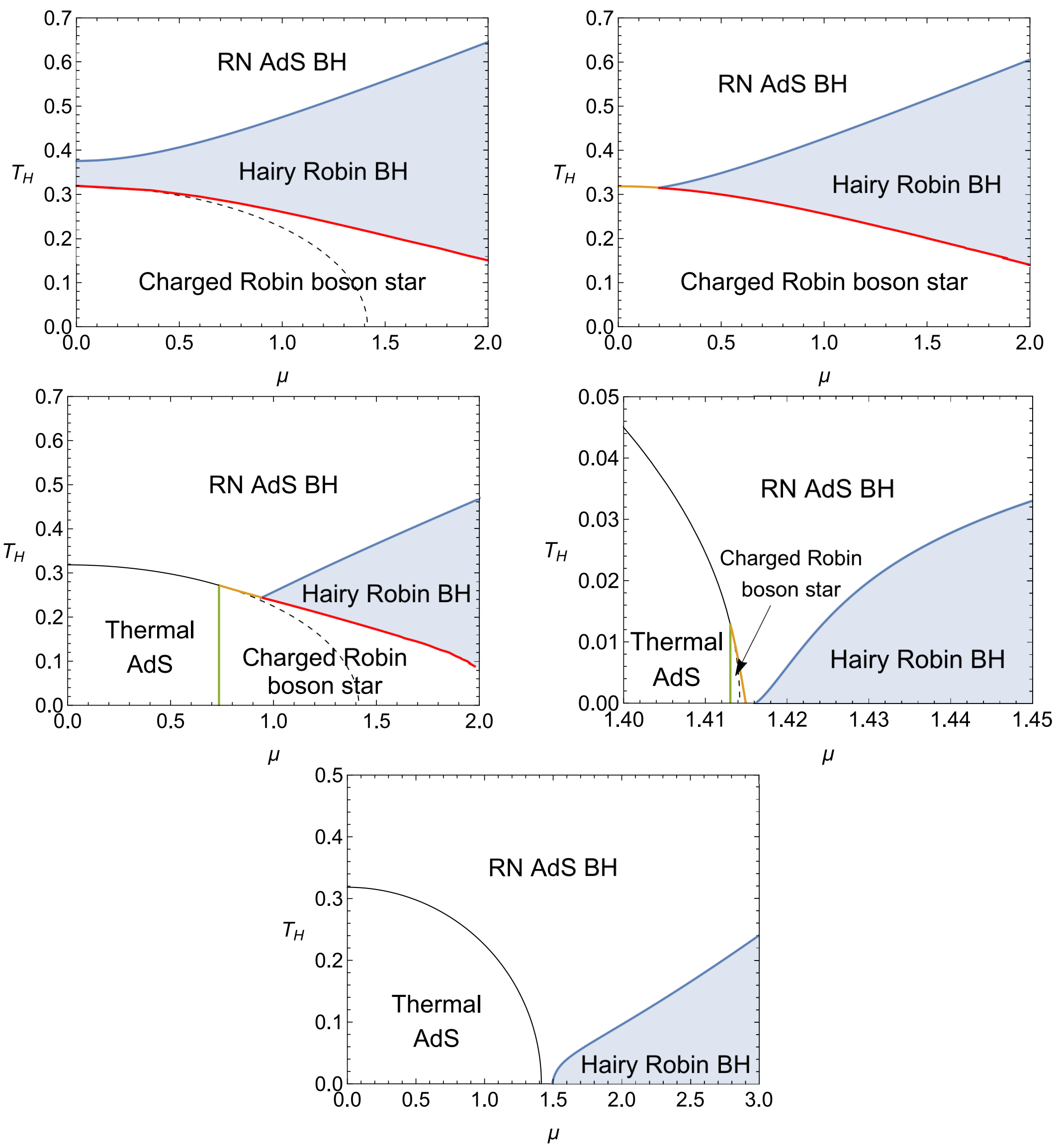

Figure 3: Phase diagram for $q = 1$ and $\zeta/\pi = 0.7, 0.682, 0.6, 0.239, 0.2$. (a) Top left: $\zeta/\pi = 0.7$; (b) Top right: $\zeta/\pi = 0.682$; (c) Middle left: $\zeta/\pi = 0.6$; (d) Middle right: $\zeta/\pi = 0.239$; (e) Bottom: $\zeta/\pi = 0.2$.